# Condensation heat transfer and pressure drop characteristics of R-600a in horizontal smooth and helically dimpled tubes

Article (Accepted Version)

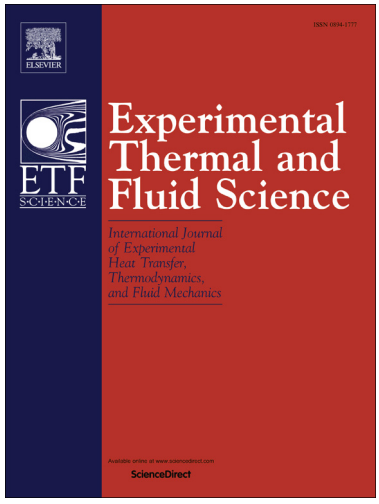


# Condensation Heat Transfer and Pressure Drop Characteristics of R-600a in Horizontal Smooth and Helically Dimpled Tubes

A. Sarmadian, M. Shafaee, H. Mashouf, S.G. Mohseni

PII: S0894-1777(17)30098-5
DOI: http://dx.doi.org/10.1016/j.expthermflusci.2017.04.001
Reference: ETF 9063

To appear in: *Experimental Thermal and Fluid Science*

Received Date: 14 March 2016
Revised Date: 13 March 2017
Accepted Date: 2 April 2017

Please cite this article as: A. Sarmadian, M. Shafaee, H. Mashouf, S.G. Mohseni, Condensation Heat Transfer and Pressure Drop Characteristics of R-600a in Horizontal Smooth and Helically Dimpled Tubes, *Experimental Thermal and Fluid Science* (2017), doi: http://dx.doi.org/10.1016/j.expthermflusci.2017.04.001

# Condensation Heat Transfer and Pressure Drop Characteristics of R-600a in Horizontal Smooth and Helically Dimpled Tubes

**A. Sarmadian[a], M. Shafaee*[a], H. Mashouf[a], S.G. Mohseni[b]**

[a]Faculty of New Sciences and Technologies, University of Tehran, Tehran, Iran

[b]Energy Institute of Higher Education, Saveh, Iran.

*Corresponding Author, Email:mshafaee@ut.ac.ir, Tel.: +98-919-0110200; fax: +98-21-88497324

## ABSTRACT

In the present study, condensation heat transfer and frictional pressure drops of refrigerant R-600a (iso-butane) inside a helically dimpled tube and a plain tube of internal diameter 8.3 mm were measured and analyzed. All tests were performed at different vapor qualities up to 0.82 and average saturation temperatures ranging between 38 and 42℃. Refrigerant mass fluxes varied in the range of 114-368 kg/m$^2$s. The inner surface of the helically dimpled tube has been designed and reshaped through three-dimensional material surface modifications consists of both shallow and deep protrusions which are placed evenly in helical directions on the tube wall. The experimental results show that the heat transfer coefficients of the dimpled tube are 1.2-2 times of those in smooth tube with a pressure drop penalty just ranging between 58% and 195%. The highest heat transfer coefficient is occurred at vapor quality of 0.53 and mass flow rate of 368 kg/m$^2$s. On the other hand, the maximum increase of pressure drop takes place at vapor quality of 0.55 and mass flow rate of 368 kg/m$^2$s.

***Keywords:*** *Condensation; Dimpled tube; R-600a; Heat transfer; Pressure drop.*

**Nomenclature**

| | |
|---|---|
| $\dot{m}$ | mass flow rate (kg/s) |
| $A$ | surface area ($m^2$) |
| $C_p$ | specific heat (kJ/kg k) |
| $D$ | diameter(mm) |
| $G$ | mass velocity ($kg/m^2s$) |
| $h$ | specific enthalpy (kJ/kg) |
| $h$ | heat transfer coefficient ($kW/m^2$ K) |
| $I$ | current (A) |
| $k$ | thermal conductivity (W/m K) |
| $L$ | length (mm) |
| $p$ | pressure (kPa) |
| $PFE$ | energy performance factor |
| $PFS$ | surface performance factor |
| $Q$ | rate of heat transfer (W) |
| $q$ | heat flux ($kW/m^2$) |
| $Re$ | Reynolds number |
| $T$ | temperature (K) |
| $V$ | voltage (V) |
| $x$ | vapor quality |

$p$ pitch ratio

Greek symbols

$\dot{v}$ volumetric flow rate ($m^3/s$)

$\Delta p$ pressure drop (kPa)

$\alpha$ void factor

$\gamma$ efficiency factor

$\rho$ density ($kg/m^3$)

$\sigma$ surface tension (N/m)

$\varpi$ power (W)

Subscripts

*D* dimpled

*f* liquid phase

*fric* frictional

*g* vapor phase

*h* heater

*i* inner

*lat* latent

*mom* momentum

*o* outer

*p* plain

*ref* refrigerant

*s* smooth

*sat* saturated

*sen* sensible

*tot* total

*tc* test condenser

*w* wall

*w* water

## 1. Introduction

The design of efficient condenser has been an important consideration to obtain energy efficiency augmentation in refrigeration and air conditioning applications. In this regard, many heat transfer enhancement technologies have been developed, including active and passive enhancement technologies. The treated surfaces, rough surfaces, extended surfaces, swirl flow devices and nanofluid are the passive methods. Micro groove tubes [1], micro-fin tubes [2], herringbone tubes [3], helically corrugated tubes [4], and inserted tubes such as modulated heat transfer tube (MHTT) [5, 6] are the enhanced condensation tubes. Recently, several passive techniques such as rough surfaces and dimples have been reviewed by Liu and Sakr [7]. Enhanced inner surfaces are commonly used because they can produce higher heat transfer coefficient with a small pressure drop penalty. Moreover, Gupta and Uniyal [8] reported that the use of dimples over the heat exchanger tube surface can be very advantageous in relation to other enhancement methods due to the simplicity of their manufacturing process and no extra cost in raw materials or labor. Recently, Kukulka and Smith [9] evaluated the relationship between heat transfer enhancement and the surface geometry of tubes which were produced by Vipertex$^{TM}$ and

have been named EHT (Enhanced Heat Transfer) tube (**Fig. 1** (a)). The inner surface of the 1EHT tube was enhanced by dimples. They compared the heat transfer for single phase flows and found that the 1EHT surface can produce heat transfer increase of more than 500% when compared to that of smooth tube. In another experimental studies, Kukulka et al. investigated the condensation and evaporation heat transfer of R410A, R22, and R32 inside [10] and outside [11] a smooth tube and a Vipertex$^{TM}$1EHT tube. The results indicated that the average evaporation and condensation heat transfer coefficients for R22, R32, and R410A in the 1EHT tube were approximately two times greater than those of a smooth tube and condensation heat transfer performance on the outside of a 1EHT tube was less than a smooth tube due to the pattern/drainage characteristics of that model of tube for the flow conditions considered. They also demonstrated pressure drop results in both single and two-phase flows. Guo et al. [12] performed an experimental investigation to evaluate convective condensation and evaporation of R22, R32, and R410A inside a smooth tube, a herringbone tube and a newly developed enhanced surface EHT tube at low mass fluxes. The inner surface of the EHT tube was enhanced by dimple/protrusion and secondary petal arrays which was produced by Vipertex$^{TM}$ too (**Fig. 1** (a)). They found out that the condensation heat transfer coefficient of the EHT tube is 1.3-1.95 times larger than a smooth tube and the herringbone tube is 2.0-3.0 times that of the smooth tube. But they didn't investigate pressure drop of these tubes.

Investigation of the influence of dimples/protrusions as a surface roughness on convective condensation is rarely reported in literatures, but its influence on single phase flow are studied extensively. Suresh et al. [13] performed an experimental investigation on the convective heat transfer and friction factor characteristics in the plain and helically dimpled tube (**Fig. 1** (b)) in single phase flow with constant heat flux and using Cuo/water nanofluid as working fluid. Their

results revealed that the Nusselt number with dimpled tube and nanofluids under turbulent flow was about 19%, 27%, and 39% higher than the Nusselt number obtained with plain tube and dimpled tube. Friction factors were about 2–10% higher than the plain tube. Recently, the application of shallow square dimples on the walls of flat tubes (**Fig. 1** (c)) in compact heat exchangers for vehicular applications was experimentally investigated by Nascimento and Garcia [14]. It was found that the use of shallow square dimples in flat tubes promoted an increase in the heat transfer augmentation factor between 1.37 and 2.28. Recently, Li et al. appraised the relationship between heat transfer enhancement and the surface geometry of a dimpled enhanced tube (**Fig. 1** (d)) using experimental and numerical simulation techniques [15]. numerical simulations were conducted to simulate geometric design optimization of enhanced tubes and were validated with experimental data [16]. Results showed that dimples on tube surface present high heat transfer performance and compared to staggered configuration, the in-line dimples arrangement provided better overall heat transfer characteristics. In addition, the geometric parameters like the shape of dimple, depth, pitch, and starts were found to have significant effects on overall heat transfer performance, while the dimple diameter has an insignificant effect on thermal performance. These literatures indicate that the use of passive methods to enhance two phase flow heat transfer performance based on the application of dimple/protrusion patterns, needs more investigation. In this regard, both shallow and deep dimples/protrusions during evaporation of R-600a inside helically dimpled tube in our previous paper [17] show a proper heat transfer augmentation, however, to the best knowledge of the authors, there is no previously study on:

- Condensation process of the refrigerant R-600a inside the tube with the enhanced geometry which is considered in this study.

- Pressure drop characteristics of R-600a in a helically dimpled tube.

The modified helically dimple pattern which was used in the present study means reshaping plain tube, so evenly placed dimples (deep and shallow ones) in the tube wall form. Thus, at the first, helical patterns of both shallow and deep dimples' direction can lead to swirling is created in the flow in areas close to the wall and finally create increased performance through a combination of: increased turbulence; boundary layer disruption; secondary flow generation and increased heat transfer surface area. Consequently, all of these can cause an increase in the heat transfer coefficient. On the other hand, due to the environmental problems by CFCs and HCFCs and obvious necessity of development of new alternative refrigerants, comparing the ozone depletion potential of R-600a (0) with R12 (1) and 100 years Global Warming Potential of R-600a (20) with R-134a (1370) shows that R-600a has a better environmental performance [18, 19]. Moreover, from the heat transfer performance point of view, some studies noted that excellent thermodynamic properties of R-600a leading to high energy efficiency. For instance, Lee et al. in an experimental study [20] discussed that R-600a has a better energy performance compared with other refrigerants. Chao-Chieh Yu and Tun-Ping Teng [21] indicated that the use of R-600a can enhance the enhancement factors (EFs) of refrigerators. Therefore, the purpose of this study is to perform an experimental investigation on the convective condensation heat transfer of R-600a inside the helically dimpled tube.

## 2. Experimental setup

The test apparatus consisted of two main closed loops: the cold-water loop and the refrigerant loop. The cold-water loop was connected to the condensers. Cold water removed the latent heat from the condensing refrigerant. The water temperature was kept constant in the range of 14-

16℃. A schematic layout of the refrigerant loop is illustrated in **Fig. 2**. The main elements are gear pump, flow meter, heaters, test condenser, sight glasses, post condenser, reservoir, thermocouples, pressure indicators, differential pressure drop transducer and necessary instruments for flow control. The gear pump (ZDF, Czech) with a variable frequency, preciously adjustable stroke and flow rate, and nominal power of 20 L/min, circulated the refrigerant and controlled the mass velocity. Two Coriolis mass flow meter (MASS/2100/6000, Danfoss, Denmark) with the accuracy within 0.1% of the full scale, were located downstream of the gear pump in both water loop and refrigerant loop to measure the water and refrigerant mass flow rates, respectively. To achieve the desired value of vapor quality at the inlet of test condenser, two AC (alternative current) 6 kW electrical resistance heaters were installed before the test section. The heaters were well insulated. Both the AC voltage and current had the uncertainties of 0.1%. Watt transducer measured power which was supplied by heaters. A platinum 100 RTD and a pressure transducer determined the enthalpy of refrigerant at the inlet of the heaters. The test condenser was a horizontal double pipe heat exchanger in which refrigerant flowing in the inner tube and water flowing in a counter-flow direction in the annulus. The length of test section is 1200 mm. Two kinds of tube were used as inner tube: one smooth and one helically dimpled tube. Both of the tubes have inner diameter of 8.3 mm, thickness of 0.6 mm and were made of copper. The geometry of helically dimpled tube is shown in **Fig. 3**. As can be seen, the dimples were arranged helically with a pitch ratio $(= p/d)$ of 1.21 on the wall of inner tube. The diameters and depths of shallow dimples were maintained at a constant value of 1 mm and 0.5 mm, respectively. On the other hand, the diameter and depth of deep dimples were maintained at constant values of 2 mm and 1 mm, respectively. The range of operating parameters in the present study is given in **Table 1**. In order to measure quasi local heat transfer coefficient, the

outside wall temperatures of inner tube were measured at five axial locations by T-type thermocouples (THERMOCOAX, China) with the accuracy of ±0.1℃. The distance between two neighboring cross sections was 200 mm. As can be seen from **Fig. 4**, at each of these axial locations, three thermocouples were welded at the top, bottom and side of the tube to take care of any circumferential temperature variations and they penetrated the corresponding branch tube for signal processing. Two calibrated RTD PT 100 temperature sensors with accuracy of ±0.1℃were located at the inlet and outlet of the shell, to measure the cooling water temperature. Inlet pressure of the test section was measured by EN 837-1 Wika model pressure gauge with the accuracy of 1 kPa, and the pressure drop along the test section was measured by a PDM-75 pressure transducer sensor with the accuracy of 0.075% of the full scale which was calibrated to measure the pressure drop in the range of 0–150 kPa. A sight glass was also mounted just after the test condenser for flow pattern visualization. The length of the sight glass is 120 mm and it has an inner diameter identical to that of the inner tube of test condenser. In order to reach the steady condition and stabilize the operating condition and to ensure that the refrigerant was liquid before entering the pump, a reservoir and a counter-flow condenser with 12 m coiled tube and cylinder shell was installed between test condenser and gear pump. The working fluid was Isobutene (R-600a) with the purity of 99.5%. The uncertainties analysis was calculated by using the method proposed by Kline and McClintock [22] and it was found that the uncertainty in the determination of condensation heat transfer coefficient is within 10% for all the test runs.

## 3. Data reduction

The experimental apparatus was installed to appraise the quasi local heat transfer coefficient and frictional pressure drop during condensation. It was assumed that the system reached to steady

state condition when temperature and pressure were constant for at least 15 minutes. Then some test is iterated two times to check the reproducibility of test apparatus. The thermodynamic and transport properties of R-600a were evaluated by commercial software (Engineering Equation Solver, EES). In order to determine a factor to account heat leakage of the heaters through the insulation, the following equation was used:

$$\gamma = \dot{m}_{ref}(h_2 - h_1)/(VI)_h \quad (1)$$

Where $\dot{m}_{ref}$, $V$, $I$, $h_2$, and $h_1$are the refrigerant mass flow rate, electric voltage, electric current, enthalpy of refrigerant at the test condenser inlet, and enthalpy of refrigerant at the heaters inlet, respectively. The measured evaporator thermal efficiency was about 0.95.

For in-tube condensation the inlet quality of test condenser was obtained by:

$$x_{in,tc} = (\gamma(VI)_h - C_p\dot{m}_{ref}(T_{sat,h,in} - T_{ref,h,in}))/\dot{m}_{ref}h_{fg,h} \quad (2)$$

Where$C_p, T_{sat,h,in}, T_{ref,h,in}$, and $h_{fg,h}$ are the specific heat of refrigerant, saturated temperature of refrigerant was taken at the average pressure of the heaters, temperature of the refrigerant at the inlet of the heaters, and vaporization enthalpy of refrigerant at the average pressure of the heaters, respectively.

The total heat transfer from the test section was calculated from an energy balance for the cooling water flowing through the annulus:

$$Q_w = C_{p,w}\dot{m}_w(T_{w,out} - T_{w,in}) \quad (3)$$

Where $Q_w, C_{p,w}, \dot{m}_w, T_{w,out},$ and $T_{w,in}$ are the total heat transferred from the test section, specific heat of water at average water temperature through the annulus, mass flow rate of water, annulus outlet temperature of water, and annulus inlet temperature of water, respectively.

The quality of refrigerant at the outlet of the test condenser $x_{out,tc}$ was calculated from an energy balance on the test condenser:

$$x_{out,tc} = x_{in,tc} - Q_w/(\dot{m}_{ref}.h_{fg,tc}) \quad (4)$$

Where $h_{fg,tc}$ is vaporization enthalpy of refrigerant at the average pressure of the test condenser.

The local vapor quality through the whole test section was obtained from:

$$x_{tc} = (x_{in,tc} + x_{out,tc})/2 \quad (5)$$

The quasi local convective heat transfer coefficient was evaluated by the following equation [23]:

$$h_{ref} = \left[\frac{\pi D_i L(T_{sat}-T_{wall})}{\dot{m}_w C_{p,w}(T_{w,out}-T_{w,in})} - \frac{D_i}{2k} ln\left(\frac{D_o}{D_i}\right)\right]^{-1} \quad (6)$$

Where $D_i, L$, $T_{sat}$, $T_{wall}$, $D_o$, and $k$ are the inner diameter of inner tube, test condenser length, saturated temperature of refrigerant at the test condenser operating pressure, wall temperature of inner tube which was the average of temperatures measured by all the thermocouples installed through the inner tube of the test condenser, outer diameter of the inner tube, and thermal conductivity of copper, respectively.

The drop pressure transducer showed the total pressure drop for horizontal tube consists of momentum pressure loss and frictional pressure loss. Momentum pressure loss was calculated from the following equation:

$$\Delta P_{mom} = G^2 \left\{\left[\frac{(1-x_{tc})^2}{\rho_f(1-\alpha)} + \frac{{x_{tc}}^2}{\rho_g \alpha}\right]_{in,tc} - \left[\frac{(1-x_{tc})^2}{\rho_f(1-\alpha)} + \frac{{x_{tc}}^2}{\rho_g \alpha}\right]_{out,tc}\right\} \quad (7)$$

Where, $\alpha$ is the void fraction. Void fraction can be calculated from the correlation developed by Steiner [24] which is applicable for different flow regimes:

$$\alpha = \frac{x_{tc}}{\rho_g}\left\{\left(1+0.12(1-x_{tc})\right)\left(\frac{x_{tc}}{\rho_g}+\frac{(1-x_{tc})}{\rho_f}\right)+\frac{1.18(1-x_{tc})[g\sigma(\rho_f-\rho_g)]^{0.25}}{G_{tot}^2{\rho_f}^{0.5}}\right\}^{-1} \quad (8)$$

For annular flow, which was the dominant flow regimes of the present study the void fraction, $\alpha$, is determined from the Zivi correlation [25], as follows:

$$\alpha = \frac{1}{1+\left(\frac{1-x_{tc}}{x_{tc}}\right)\left(\frac{\rho_g}{\rho_l}\right)^{2/3}} \quad (9)$$

Finally, by subtracting the momentum pressure loss from total pressure loss which was read by pressure drop transducer, the frictional pressure loss was calculated.

## 4. Results and discussion

In this section heat transfer coefficients and frictional pressure drops during condensation inside the smooth tube and a dimpled tube and their performance factors are discussed in separate subsections as follows:

### *4.1. Heat transfer*

First of all, as shown in **Fig. 5**, the experimental heat transfer coefficients of smooth tube were compared with those predicted by Thome et al. [26] and Cavalini et al. [27] which were proposed for Hydrocarbon refrigerants. As was stated in [26], the heat transfer model based on flow regimes can predict local condensation heat transfer coefficients for all of the following flow regimes; annular, intermittent, stratified-wavy, fully stratified and mist flow. Therefore, as it

could be expected, more than 90% of all the points are inside ±20% error window. The correlation of Cavalini et al. [27] produces 56% of experimental data (those are related to fully stratified and stratified-wavy flow pattern regions) inside ±20% error window. It should be noticed that annular, intermittent, and stratified-wavy flow were recognized for plain tube, whereas there was no stratified-wavy flow in flow pattern visualization of the dimpled tube.

**Fig. 6** depicts the full set of experimental results of the heat transfer coefficient versus vapor quality at mass fluxes of 114, 155, 270 and 368$kg/m^2s$. The test section was kept constant at average saturation temperatures ranging between 38 and 42℃ for all vapor qualities. Results comprehensively grouped together in the same plot, allowing to easily identify the effects of dimpled tube application. It is observed that the application of dimples/protrusions inside the test condenser tube has produced higher heat transfer coefficient compared to smooth tube value. The magnitude of the augmentation is a complex function of mass velocity and vapor quality. It can be observed that the dimpled tube enhances the heat transfer coefficient in a range of 20% to 100% in comparison to those for the smooth tube. This is because the dimpled tube has a significant effect on mixing of the condensate film at the tube wall and increasing the turbulent flow. The helically dimpled surface alters the flow field in a circular tube in several different ways. The blockage and partitioning of the flow cross section by the finite-thickness protrusion increase the axial velocity and the wetted perimeter. The partitioned, helically twisting duct also provides a longer effective flow path and imposes a curvature-induced transverse force on the axial flow to produce secondary circulation. Of these, the dominant flow mechanism is the generation of swirl, which causes a transverse fluid transport across the protrusion-partitioned duct cross section. This promotes greater fluid mixing and higher heat transfer coefficients; of course, the associated friction penalty also increases. The secondary circulation also produces

greater thermal mixing, which results in higher heat transfer coefficients. Therefore, that higher heat transfer coefficient is obtained due to tube partitioning, blockage, and flow acceleration and helical swirl generation. Furthermore, the large radial acceleration induced by helically dimpled surface causes the bubbles to migrate to the center of the tube, resulting in rapid condensation of the vapor while in axial flow (smooth tube flow), the bubbles remain near the heated surface, condensing rather slowly as they are swept downstream. At vapor qualities range from 0.3 to 0.5 the heat transfer coefficient augmentation is more significant. This phenomenon is due to the fact that as vapor quality decreases, the transition from annular flow to intermittent flow for smooth tube occurs in region which is distinguished by an ellipse in **Fig. 6**, and the dimples delay this transition as can be seen from the visualization images which are placed in the **Fig. 6**. This phenomenon enhances the heat transfer coefficient of dimpled tube relative to the smooth tube. This behavior are very similar to behavior that was reported previously for herringbone and smooth tubes by Olivier et al. [28]. For all mass fluxes, the lowest heat transfer coefficient ratio takes place at vapor qualities higher than 0.5. This is because of that, as the vapor quality increases the density of flow decreases, thus the velocity of the flow increases which cause an increase in turbulence and as the turbulence of flow increases the influence of dimples/protrusions on flow separation, boundary layer disruption, and flow mixing gets weaker.

In **Fig. 7** the variation of heat transfer coefficient with vapor quality for dimpled tube at the lowest experimented mass flux of 114 $kg/m^2s$ and the highest mass flux of 368 $kg/m^2s$ is illustrated. As can be seen, the mass flux has a noticeable effect on heat transfer coefficient. Condensation heat transfer coefficients at mass flux of 368 $kg/m^2s$ are about 1.9-2.8 times those of the mass flux of 114 $kg/m^2s$. The highest heat transfer ratio takes place at vapor quality of 0.11 and the lowest one happens at vapor quality of 0.55. **Fig. 7** also depicts that as

vapor quality increases the heat transfer ratio of two mass fluxes decreases.

Moreover, as expected the heat transfer coefficient increases continuously with vapor quality and this is due to the heat transfer augmentation that occurs at higher qualities where flow has higher velocity. For annular flow a thin liquid layer spread along the periphery of the tube. As vapor quality increases the liquid film layer becomes thinner with the lower resistance to heat transfer increasing.

*4.2. Pressure drop*

First of all, comparison was made between the experimental data for the frictional pressure drop inside the smooth tube with the predicted values of Friedel [29]. For this purpose, pressure loss was measured at four different mass velocities (114-368kg/m²s) with the vapor quality varied within the range of 0.1-0.82. In **Fig. 8**, it can be observed that the correlation of Friedel [29] predicts more than 80% of the experimental pressure drop data of the present investigation within an error range of +21 to -25% and the rest of the points are contained inside -25% to -50% error window.

**Fig. 9** shows the variation of frictional pressure drop with vapor quality for smooth and dimpled tubes at four different mass fluxes. For all mass fluxes and all vapor qualities, the frictional pressure drop of dimpled tube is higher than that of smooth tube and these relative changes are about the same either at low or high vapor qualities. This is mainly caused by the increase in friction that the dimples/protrusions bring about, flow blockage due to area reduction, turbulence augmentation, and rotational flow produced by the helically dimpled surface of the tube. As vapor quality increases the frictional pressure drop ratio of dimpled tube relative to the smooth tube increases and for all mass fluxes the highest friction pressure drop ratio occurs at highest vapor quality. The highest pressure drop of dimpled tube is 2.93, 2.9, 2.95 and 1.68 times that of

the smooth tube for mass fluxes of 114 $kg/m^2s$, 155$kg/m^2s$, 270$kg/m^2s$, and 368$kg/m^2s$, respectively.

Variations of frictional pressure drop versus vapor quality at four mass fluxes of 114 $kg/m^2s$, 155$kg/m^2s$, 270$kg/m^2s$, and 368$kg/m^2s$ for dimpled tube are collected together in **Fig. 10**. It is obvious that the frictional pressure drop at constant vapor quality increases with the mass flux. This is because of that the higher mass flux will increase the vapor velocity. Therefore, the shear stress at the interface of the liquid film and vapor increases; as a consequent the frictional pressure drop increases. At lower mass fluxes which is described by the onset and growth of swirl flow that is superimposed over the axial flow; a competing balance among convective inertia, viscous, and dimple-helical curvature-induced forces establishes swirl generation and as mass flux increases swirl which is induced by helically dimpled surface is completely established, which grows into counter rotating helical vortices and produces much higher frictional loss. In addition, it can be observed from **Fig. 10** that the frictional pressure drop at mass flux of 368$kg/m^2s$ is about 8.22 to 10 times that of mass flux of 114 $kg/m^2s$ at vapor quality of 0.52 and 0.1, respectively. This implies that as vapor quality increases the effect of mass flux on frictional pressure drop increase becomes stronger. This behavior shows a nonlinear relation between the frictional pressure drop and flow rate.

*4.3. Performance analysis*

A performance factor (*PF*) is generally used as a measure and criteria of the heat transfer enhancement technique. As we all know, the heat transfer coefficient and pressure drop are independent parameters which are not related by an equation. Thus, considering the need of the third parameter which relates to both of them and can produce the suitable condition for this purpose, Agrawal and Verma [30] proposed the ratio of pumping power to enhanced heat

transfer rate or enhanced heat transfer coefficient as an alternative to be used as the benchmark of performance evaluation. The increased pumping power due to the presence of dimples can be calculated by multiplying the volumetric flow rate, $\dot{v}$, and produced pressure drop, $\Delta P$, in the test condenser. Therefore, the pump power can be calculated from following equation:

$$\varpi = \dot{v}\Delta P \tag{10}$$

In the present work, the ratio of the power consumption of pump to heat transfer coefficient of plain flow$(\varpi/h)_p$ is calculated and then the same ratio for dimpled tube $(\varpi/h)_D$ is computed. Finally, the ratio from plain flow is divided by that for the flow with dimple, which can be considered as energy performance factor *PFE*:

$$\frac{(\frac{\dot{v}\Delta P}{h})_p}{(\frac{\dot{v}\Delta P}{h})_D} = \frac{(\frac{h_D}{h_p})}{(\frac{(\Delta P)_D}{(\Delta P)_p})} = \frac{R_h}{R_{\Delta P}} \tag{11}$$

Where$R_h$ is the ratio of dimpled tube heat transfer coefficient to plain tube heat transfer coefficient and $R_{\Delta P}$ is the ratio of dimpled tube pressure loss to plain tube pressure loss. If $R_h/R_{\Delta P}$ is greater than one, using the dimpled tube is beneficial, otherwise utilizing the dimpled tube is not recommended except for specific conditions and particular applications.

**Fig. 11** illustrates this ratio for four different mass fluxes at four vapor qualities of $x$ = 0.2, $x$ = 0.3, $x$ = 0.4, and $x$ = 0.55. from this figure, it is clear that for all conditions the *PFE* is lower than unity and all the points place between 0.5 and 1. As mentioned before, it's undesirable. However, observation also reveals that the *PFE* at constant vapor quality of $x$ = 0.2, goes toward unity by increasing the mass flux and it has a better performance relative to other vapor qualities. No consistency observed in variation of *PFE* with mass flux at $x$ = 0.3, $x$ = 0.4, and $x$ = 0.55.

On the other hand, there is another point of view to consider the effect of surface area increase of dimpled tube which is 1.084 times that of smooth tube. In this regard, surface performance factor (*PFS*) was used. This performance factor is defined as the ratio of the average heat transfer coefficient of the enhanced tube to that of nominal plain tube with consideration of the area enhancement ratio, as given by Equation bellow:

$$PFS = \frac{h_D}{h_p} . \frac{A_p}{A_D} \quad (12)$$

As can be seen from **Fig. 12** all the *PFS* values are larger than unity which is desirable. The highest and lowest values of *PFS* are 1.63 and 1.02 which are related to mass flow rate of $270 kg/m^2 s$ at $x = 0.3$ and mass flow rate of $368 kg/m^2 s$ at $x = 0.55$, respectively. Overall, it can be seen at low vapor qualities both of *PFE* and *PFS* reveal better performance. As a conclusion, this pattern of dimpled tube can use in special cases when the compact heat exchangers are required and it can be justifiable for the shortage of space, and more pumping power.

## 5. Conclusions

An experimental apparatus has been installed for evaluating the heat transfer coefficients and pressure drops during condensation of R-600ainside a helically dimpled tube and a smooth tube. The experimental tests are carried out by varying the vapor quality within the range of 0.1 - 0.82 and the refrigerant mass flux within the range of 114 - 368 $kg/m^2 s$ and the following conclusion can be drawn:

- The heat transfer coefficient and frictional pressure drop grows up with increase of vapor quality and mass flux, during condensation inside the dimpled tube.

- The heat transfer coefficients of dimpled tube were 20-100% higher than those of plain tube.
- In dimpled tube the transition from intermittent to annular regime took place at lower vapor quality than plain tube.
- The frictional pressure drops of dimpled tube were about 1.58-2.95 times those of smooth tube.
- The highest frictional pressure drop ratio took place at highest mass flux and vapor quality and the lowest frictional pressure drop ratio happened at lowest mass flux and vapor quality.
- The *PFE* values of dimpled tube were lower than unity while the *PFS* values were higher than unity and hence utilizing of dimpled tube in design of compact heat exchangers seems more beneficial.

**References**

[1] D. Graham, J. Chato, T. Newell, Heat transfer and pressure drop during condensation of refrigerant 134a in an axially grooved tube, International journal of heat and mass transfer, 42 (1999) 1935-1944.
[2] A. Cavallini, D. Del Col, L. Doretti, G. Longo, L. Rossetto, Heat transfer and pressure drop during condensation of refrigerants inside horizontal enhanced tubes, International Journal of Refrigeration, 23 (2000) 4-25.
[3] A. Miyara, Y. Otsubo, Condensation heat transfer of herringbone micro fin tubes, International journal of thermal sciences, 41 (2002) 639-645.
[4] S. Laohalertdecha, S. Wongwises, Condensation heat transfer and flow characteristics of R-134a flowing through corrugated tubes, International Journal of Heat and Mass Transfer, 54 (2011) 2673-2682.
[5] J. Xie, J. Xu, Y. Cheng, F. Xing, X. He, Condensation heat transfer of R245fa in tubes with and without lyophilic porous-membrane-tube insert, International Journal of Heat and Mass Transfer, 88 (2015) 261-275.
[6] Z. Cao, J. Xu, Modulated heat transfer tube with short conical-mesh inserts: A linking from microflow to macroflow, International Journal of Heat and Mass Transfer, 89 (2015) 291-307.
[7] S. Liu, M. Sakr, A comprehensive review on passive heat transfer enhancements in pipe exchangers, Renewable and sustainable energy reviews, 19 (2013) 64-81.

[8] A. Gupta, M. Uniyal, Review of heat transfer augmentation through different passive intensifier methods, IOSR Journal of Mechanical and Civil Engineering (IOSRJMCE) ISSN, (2012) 2278-1684.
[9] D.J. Kukulka, R. Smith, Thermal-hydraulic performance of Vipertex 1EHT enhanced heat transfer tubes, Applied Thermal Engineering, 61 (2013) 60-66.
[10] D.J. Kukulka, R. Smith, W. Li, Comparison of tubeside condensation and evaporation characteristics of smooth and enhanced heat transfer 1EHT tubes, Applied Thermal Engineering, 89 (2015) 1079-1086.
[11] D.J. Kukulka, R. Smith, W. Li, Comparison of condensation and evaporation heat transfer on the outside of smooth and enhanced 1EHT tubes, Applied Thermal Engineering, (2016).
[12] S.-p. Guo, Z. Wu, W. Li, D. Kukulka, B. Sundén, X.-p. Zhou, J.-j. Wei, T. Simon, Condensation and evaporation heat transfer characteristics in horizontal smooth, herringbone and enhanced surface EHT tubes, International Journal of Heat and Mass Transfer, 85 (2015) 281-291.
[13] S. Suresh, M. Chandrasekar, S.C. Sekhar, Experimental studies on heat transfer and friction factor characteristics of CuO/water nanofluid under turbulent flow in a helically dimpled tube, Experimental Thermal and Fluid Science, 35 (2011) 542-549.
[14] I.P. Nascimento, E.C. Garcia, Heat transfer performance enhancement in compact heat exchangers by using shallow square dimples in flat tubes, Applied Thermal Engineering, 96 (2016) 659-670.
[15] M. Li, T.S. Khan, E. Al-Hajri, Z.H. Ayub, Single phase heat transfer and pressure drop analysis of a dimpled enhanced tube, Applied Thermal Engineering, 101 (2016) 38-46.
[16] M. Li, T.S. Khan, E. Al Hajri, Z.H. Ayub, Geometric optimization for thermal–hydraulic performance of dimpled enhanced tubes for single phase flow, Applied Thermal Engineering, 103 (2016) 639-650.
[17] M. Shafaee, H. Mashouf, A. Sarmadian, S. Mohseni, Evaporation heat transfer and pressure drop characteristics of R-600a in horizontal smooth and helically dimpled tubes, Applied Thermal Engineering, 107 (2016) 28-36.
[18] M.J. Molina, F.S. Rowland, Stratospheric sink for chlorofluoromethanes: chlorine atom-catalysed destruction of ozone, Nature, 249 (1974) 810-812.
[19] M.J. Kurylo, The chemistry of stratospheric ozone: its response to natural and anthropogenic influences, International journal of refrigeration, 13 (1990) 62-72.
[20] H.-S. Lee, J.-I. Yoon, J.-D. Kim, P. Bansal, Characteristics of condensing and evaporating heat transfer using hydrocarbon refrigerants, Applied thermal engineering, 26 (2006) 1054-1062.
[21] C.-C. Yu, T.-P. Teng, Retrofit assessment of refrigerator using hydrocarbon refrigerants, Applied Thermal Engineering, 66 (2014) 507-518.
[22] S.J. Kline, F. McClintock, Describing uncertainties in single-sample experiments, Mechanical engineering, 75 (1953) 3-8.
[23] S. Said, N. Azer, Heat transfer and pressure drop during condensation inside horizontal finned tubes, ASHRAE Transactions, 89 (1983) 114-134.
[24] D. Steiner, VDI-Wärmeatlas (VDI Heat Atlas), Verein Deutscher Ingenieure, VDI-Gesellschaft Verfahrenstechnik und Chemieingenieurwesen (GCV), Düsseldorf, (1993).
[25] S.M. Zivi, Estimation of Steady-State Steam Void-Fraction by Means of the Principle of Minimum Entropy Production, Journal of Heat Transfer, 86 (1964) 247-251.
[26] J.R. Thome, J. El Hajal, A. Cavallini, Condensation in horizontal tubes, part 2: new heat transfer model based on flow regimes, International Journal of Heat and Mass Transfer, 46 (2003) 3365-3387.
[27] A. Cavallini, D.D. Col, L. Doretti, M. Matkovic, L. Rossetto, C. Zilio, G. Censi, Condensation in horizontal smooth tubes: a new heat transfer model for heat exchanger design, Heat Transfer Engineering, 27 (2006) 31-38.
[28] J.A. Olivier, L. Liebenberg, J.R. Thome, J.P. Meyer, Heat transfer, pressure drop, and flow pattern recognition during condensation inside smooth, helical micro-fin, and herringbone tubes, International Journal of Refrigeration, 30 (2007) 609-623.

[29] L. Friedel, Improved friction pressure drop correlations for horizontal and vertical two-phase pipe flow, in: European two-phase flow group meeting, Paper E, 1979, pp. 1979.
[30] K. Agrawal, H. Varma, Experimental study of heat transfer augmentation versus pumping power in a horizontal R12 evaporator, International journal of refrigeration, 14 (1991) 273-281.

## Figure captions list

**Fig. 1** Application of dimples on the surface of enhanced tubes: a) VipertexTM 1EHT [9-11] and EHT [12] tubes, b) Schematic of dimple tube by Suresh et al. [13], c) Square dimple geometry in a flat tube by Nascimento and Garcia [14], and d) Cross section and outer surface of dimpled enhanced tube by Li et al. [15]

**Fig. 2** Schematic diagram of experimental facilities with p-h diagram

**Fig. 3** Helically dimpled tube illustration and its pattern characteristics.

**Fig. 4** Details of the test section

**Fig. 5** Comparison of experimental and predicted condensation heat transfer coefficient in the smooth tube.

**Fig. 6** Heat transfer coefficient at: a) G = 114 $kg/m^2s$, b) G = 155 $kg/m^2s$, c) G = 270 $kg/m^2s$, and d) G = 368 $kg/m^2s$

**Fig. 7** The variation of heat transfer coefficient with vapor quality for four different mass fluxes of 114$kgm2s$, 155 $kg/m^2s$, 270$kgm2s$, and 368 $kg/m^2s$.

**Fig. 8** Comparison of experimental and predicted frictional pressure drop in the smooth tube during condensation.

**Fig. 9** Frictional pressure drop at: a) G = 114 $kg/m^2s$, b) G = 155 $kg/m^2s$, c) G = 270 $kg/m^2s$, and d) G = 368 $kg/m^2s$

**Fig. 10** The variation of frictional pressure drop with vapor quality for four different mass fluxes of 114$kgm2s$, 155 $kg/m^2s$, 270$kgm2s$, and 368 $kg/m^2s$.

**Fig. 11** PFE performance factor for the dimpled tube.

**Fig. 12** PFS performance factor for the dimpled tube.

## Table caption list

**Table 1** Values of the operating parameters in the present study

**Table 1.** Values of the operating parameters in the present study.

| Parameter | Value |
|---|---|
| Refrigerant | R-600a |
| Inside diameter | 8.3(mm) |
| Thickness | 0.6(mm) |
| Refrigerant mass velocity | 114-368(kg/m$^2$ s) |
| Vapor quality | 0.1-0.82 |
| Cooling water temperature | 14-16℃ |
| Average pressure | 5.3 (bar) |
| Saturation temperature | 38-42℃ |

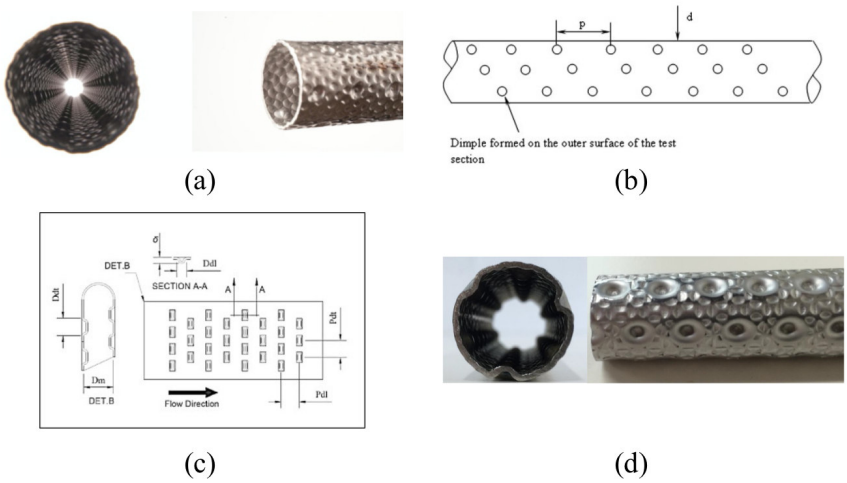


**Fig. 1.** Application of dimples on the surface of enhanced tubes: a) Vipertex$^{TM}$ 1EHT [9-11] and EHT [12] tubes, b) Schematic of dimple tube by Suresh et al. [13], c) Square dimple geometry in a flat tube by Nascimento and Garcia [14], and d) Cross section and outer surface of dimpled enhanced tube by Li et al. [15]

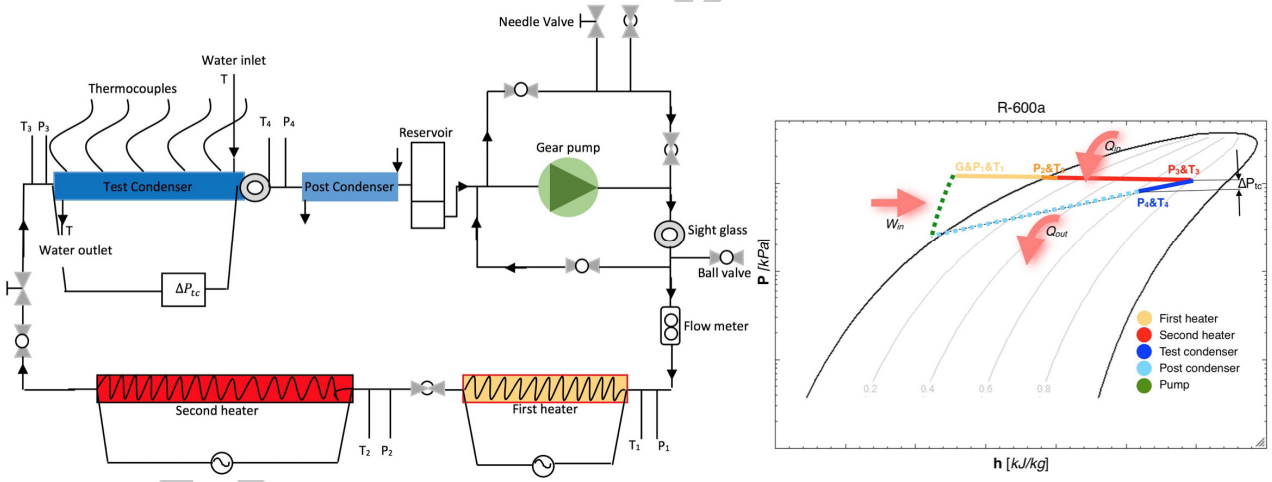


**Fig. 2.** Schematic diagram of experimental facilities with p-h diagram

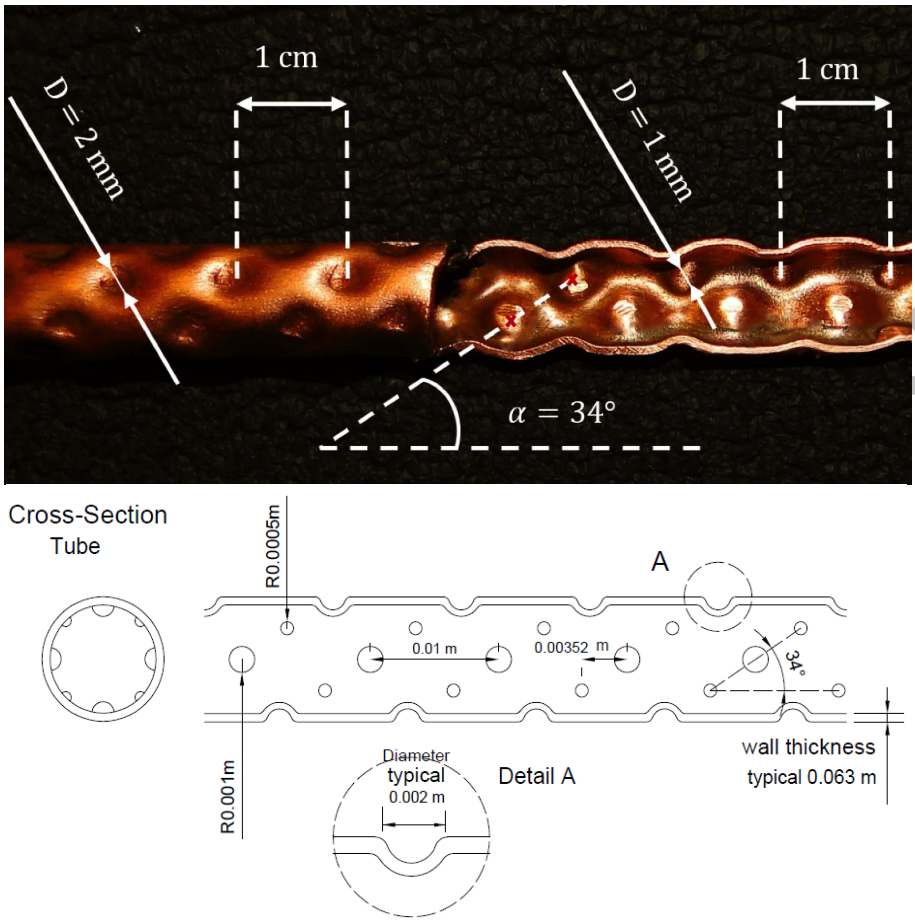


**Fig. 3.** Helically dimpled tube illustration and its pattern characteristics.

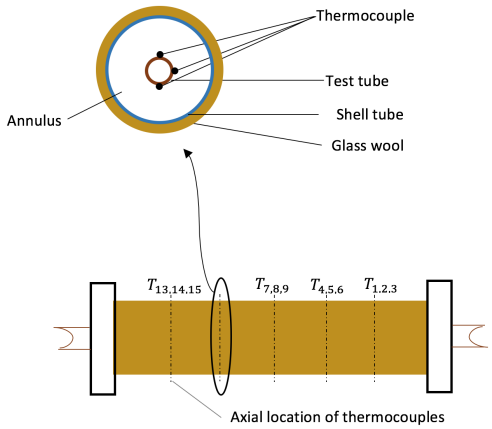


**Fig. 4.** Details of the test section

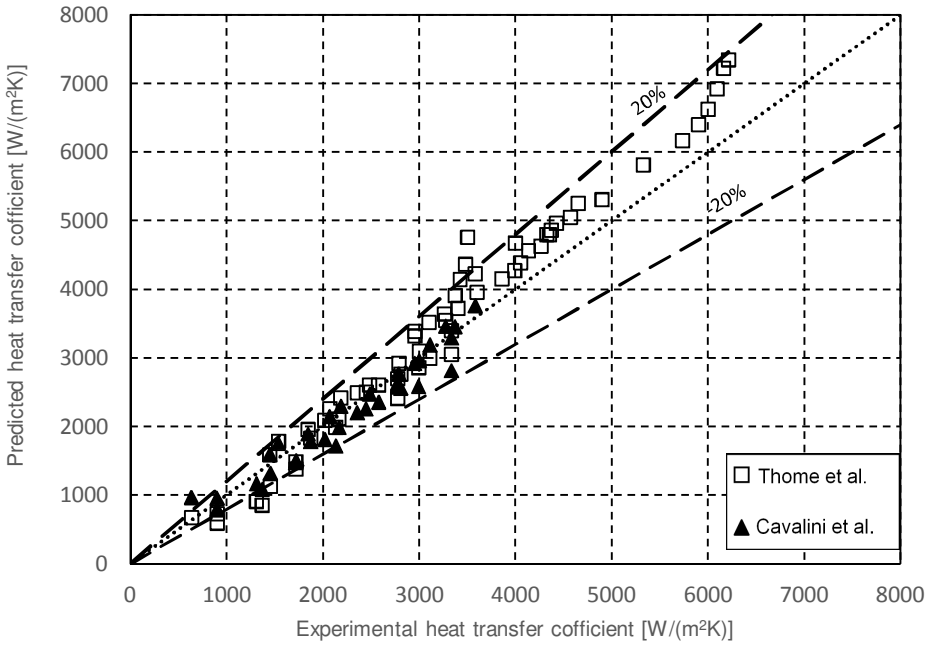


**Fig. 5.** Comparison of experimental and predicted condensation heat transfer coefficient in the smooth tube.

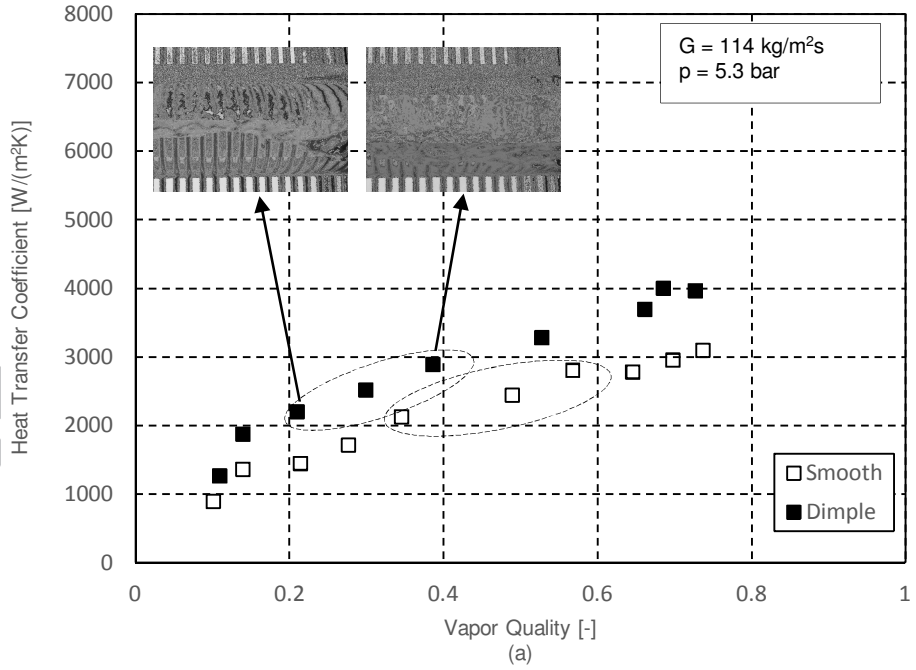


(a)

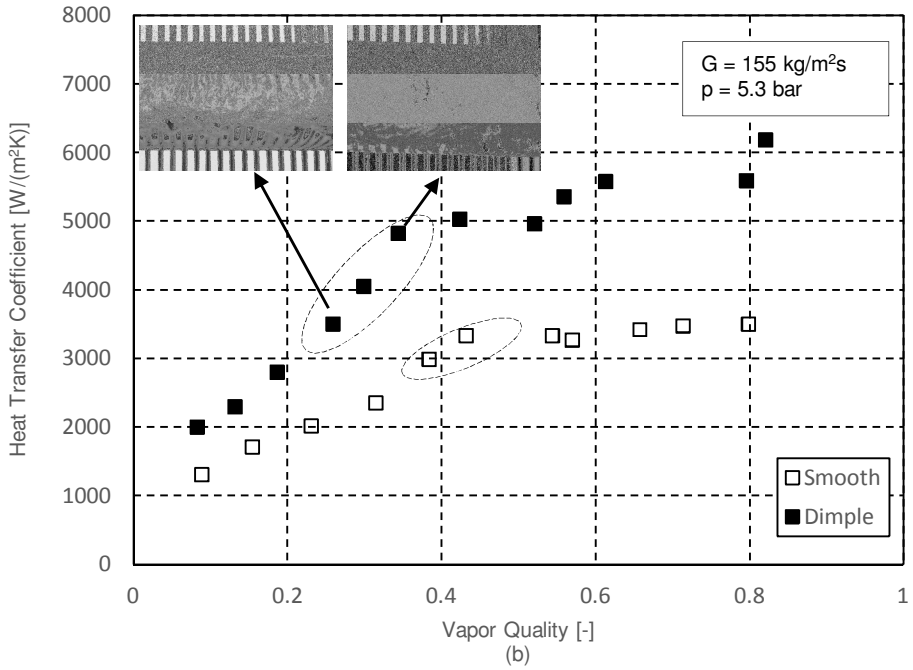


(b)

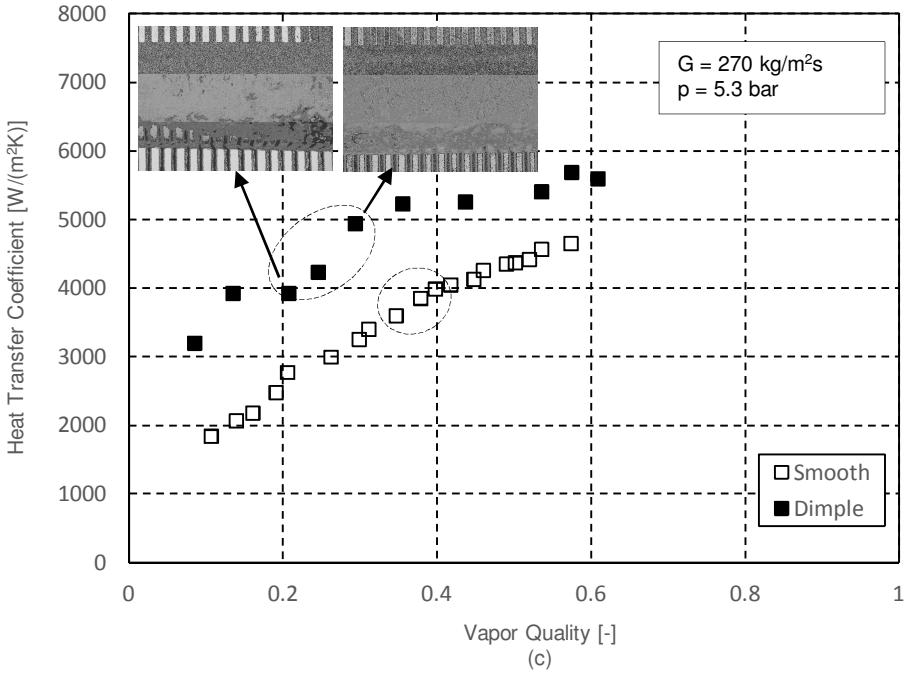


(c)

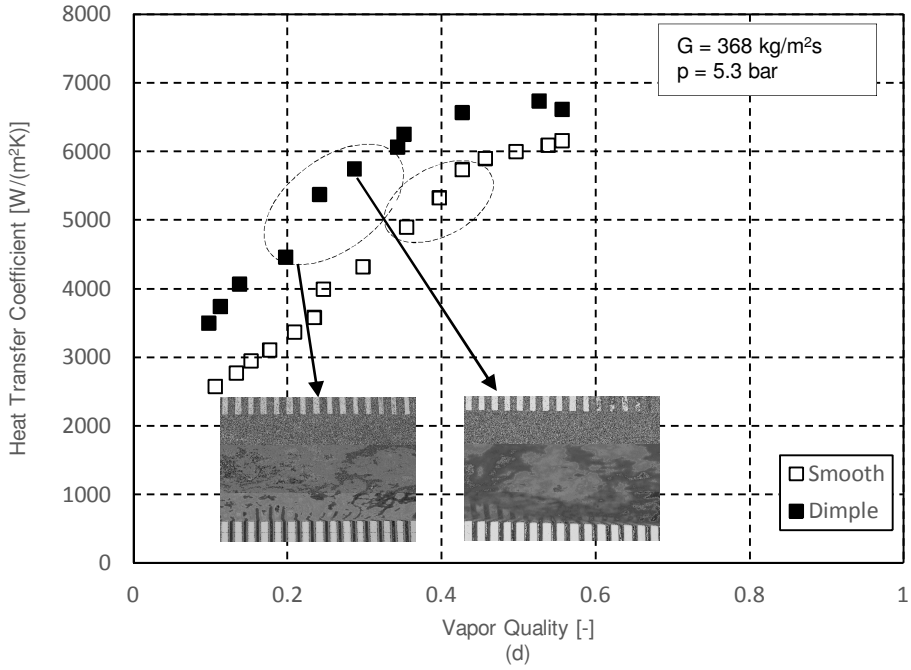


**Fig. 6.** Heat transfer coefficient at: a) $G = 114\ kg/m^2s$, b) $G = 155\ kg/m^2s$, c) $G = 270\ kg/m^2s$, and d) $G = 368\ kg/m^2s$

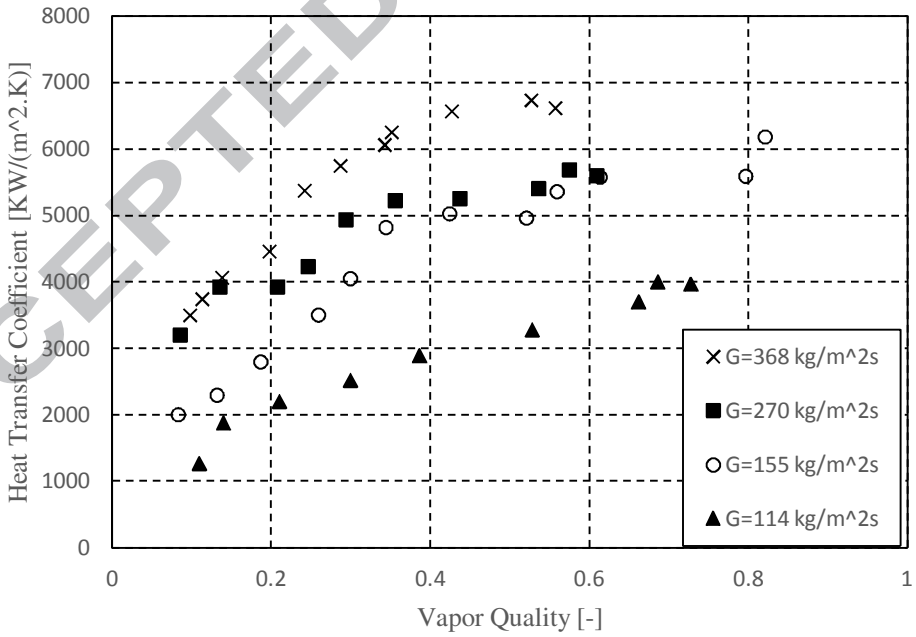


**Fig. 7.** The variation of heat transfer coefficient with vapor quality for four different mass fluxes of $114kg/m^2s$, $155\ kg/m^2s$, $270kg/m^2s$, and $368\ kg/m^2s$.

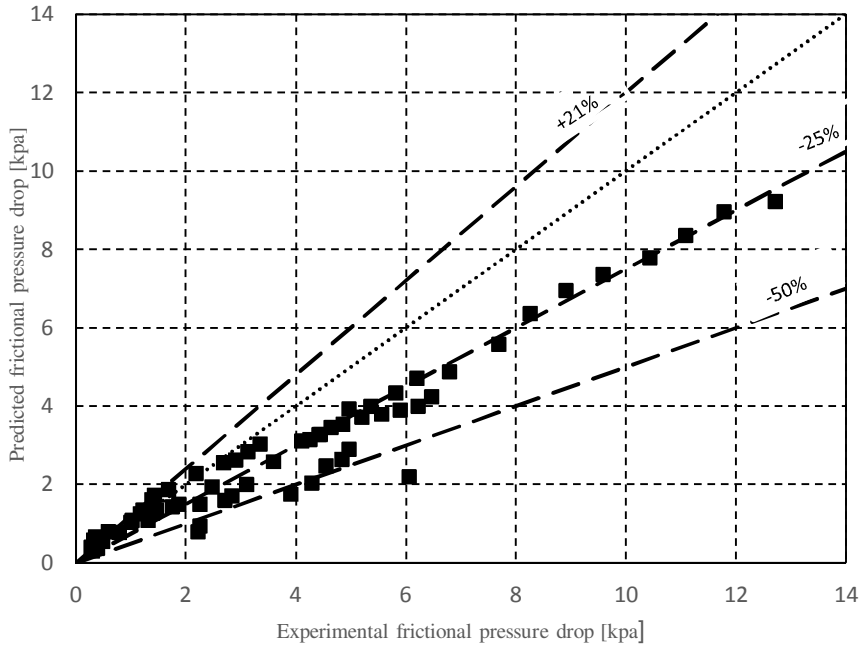


**Fig. 8.** Comparison of experimental and predicted frictional pressure drop in the smooth tube during condensation.

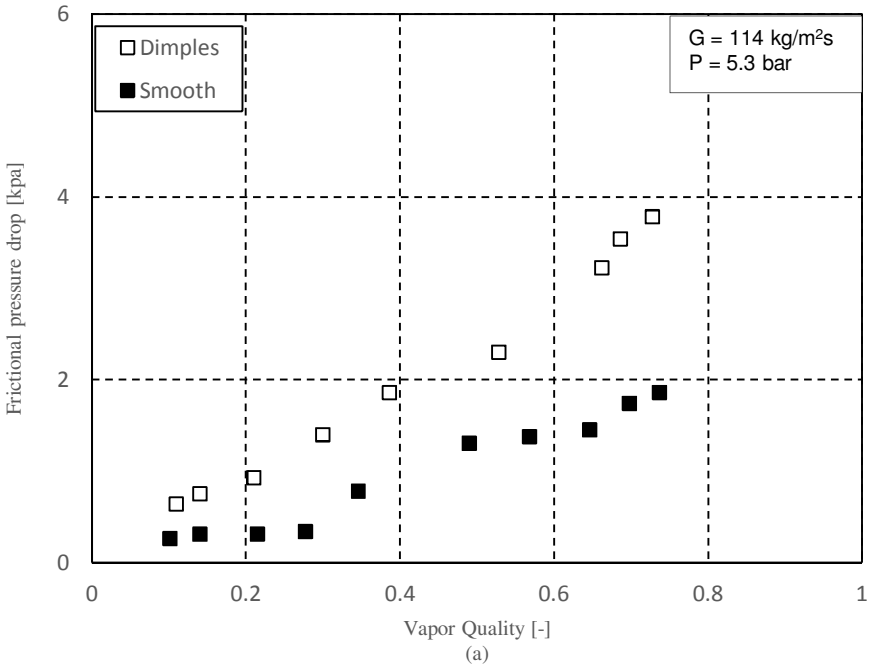


(a)

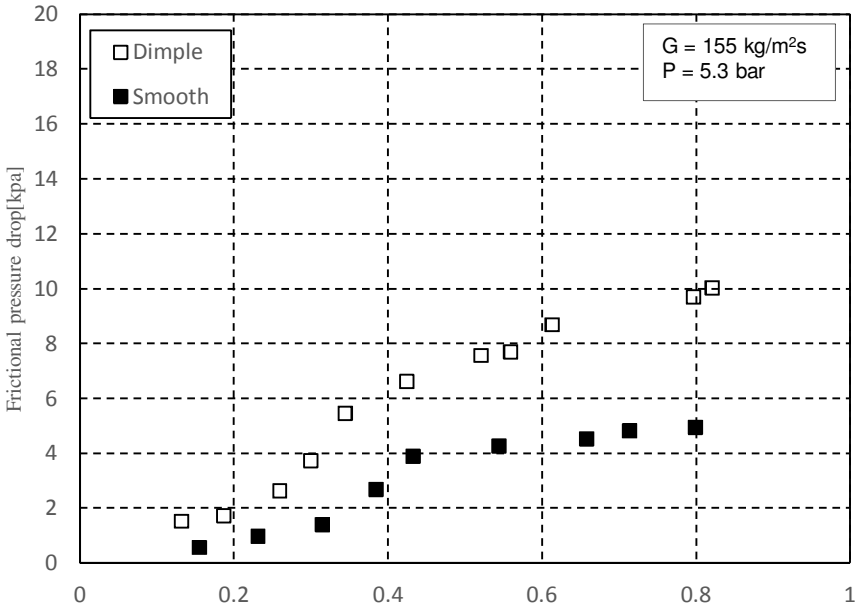


(b)

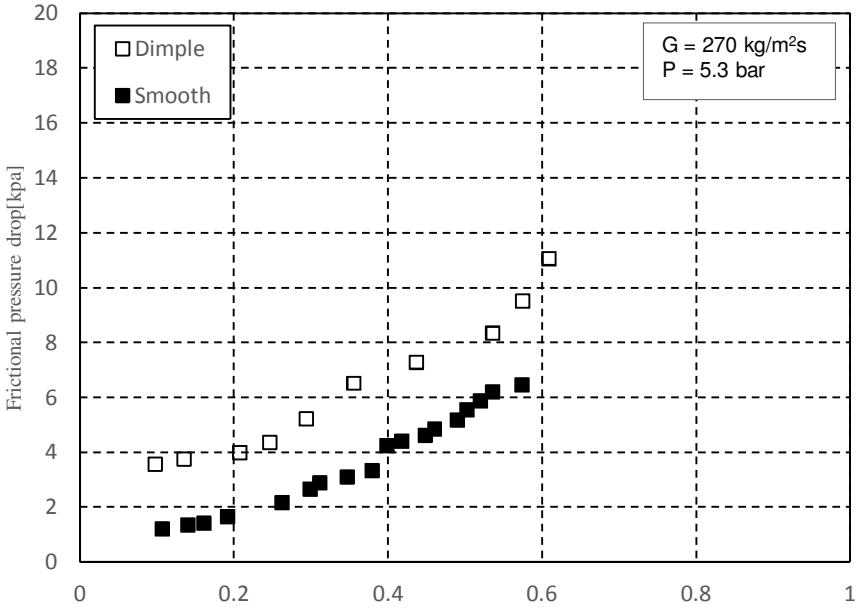


(c)

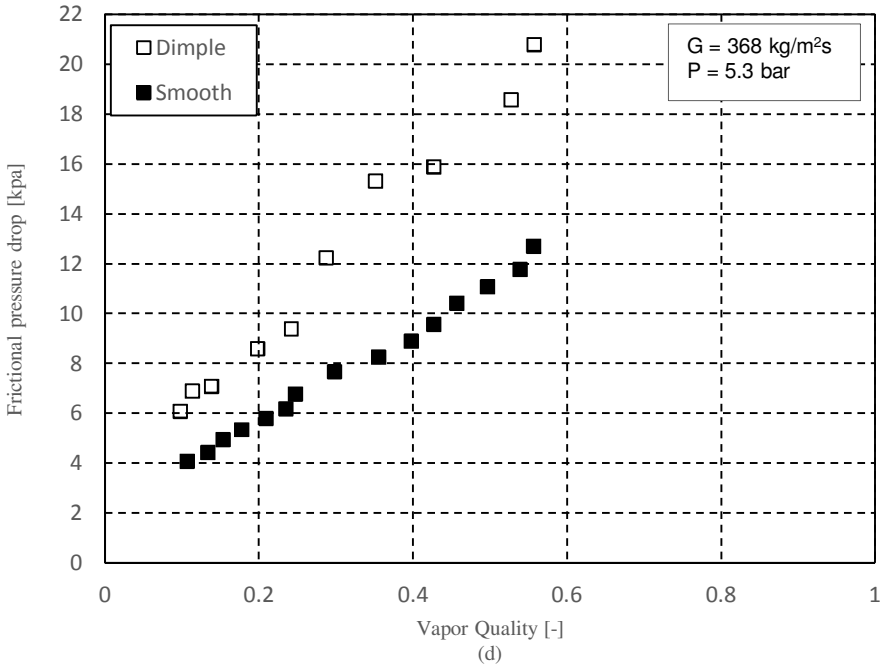


(d)

**Fig. 9.** Frictional pressure drop at: a) $G = 114\ kg/m^2s$, b) $G = 155\ kg/m^2s$, c) $G = 270\ kg/m^2s$, and d) $G = 368\ kg/m^2s$

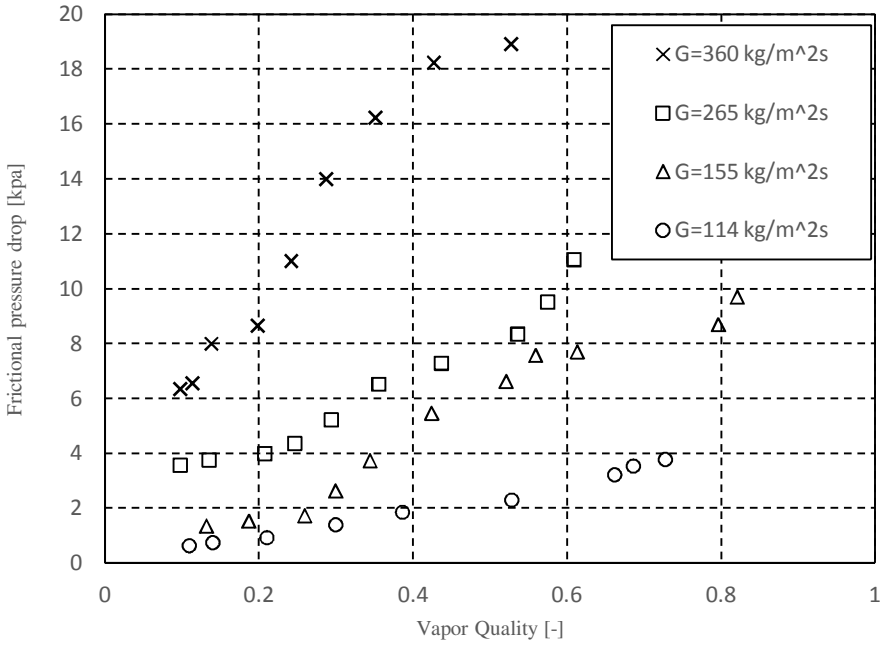


**Fig. 10.** The variation of frictional pressure drop with vapor quality for four different mass fluxes of $114 kg/m^2 s$, $155\ kg/m^2 s$, $270 kg/m^2 s$, and $368\ kg/m^2 s$.

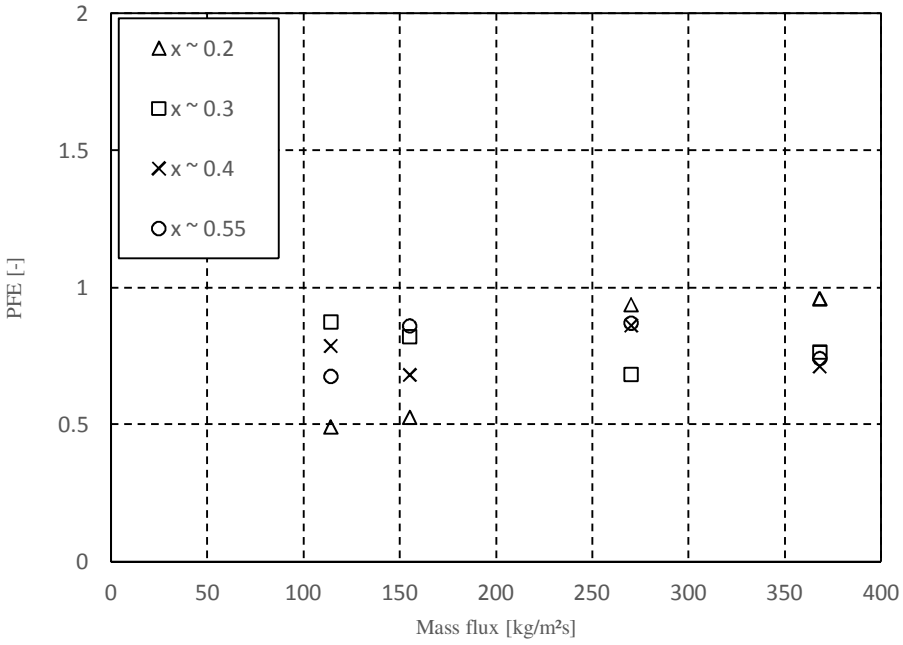


**Fig. 11.** *PFE* performance factor for the dimpled tube.

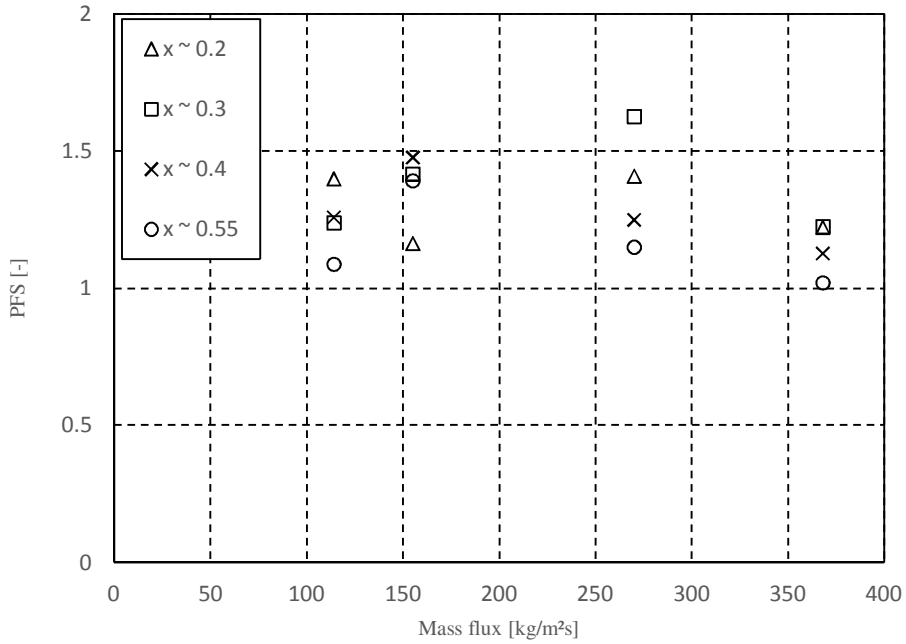


**Fig. 12.** *PFS* performance factor for the dimpled tube.

## Highlights

- Heat transfer coefficient and pressure drop in dimpled tube are considered together.
- The use of dimpled tube will improve the heat transfer augmentation factor.
- Annular to intermittent transition of dimpled tube took place in lower vapor quality.
- Dimpled tube utilizing is beneficial in compact heat exchangers design.